

Learning a Gaussian Mixture Model from Imperfect Training Data for Robust Channel Estimation

Benedikt Fesl, Nurettin Turan, *Student Member, IEEE*, Michael Joham, *Member, IEEE*,
and Wolfgang Utschick, *Fellow, IEEE*

Abstract—In this letter, we propose a Gaussian mixture model (GMM)-based channel estimator which is learned on imperfect training data, i.e., the training data is solely comprised of noisy and sparsely allocated pilot observations. In a practical application, recent pilot observations at the base station (BS) can be utilized for training. This is in sharp contrast to state-of-the-art machine learning (ML) techniques where a reference dataset consisting of perfect channel state information (CSI) labels is a prerequisite, which is generally unaffordable. In particular, we propose an adapted training procedure for fitting the GMM which is a generative model that represents the distribution of all potential channels associated with a specific BS cell. To this end, the necessary modifications of the underlying expectation-maximization (EM) algorithm are derived. Numerical results show that the proposed estimator performs close to the case where perfect CSI is available for the training and exhibits a higher robustness against imperfections in the training data as compared to state-of-the-art ML techniques.

Index Terms—Robust channel estimation, imperfect data, generative model, Gaussian mixture, OFDM system.

I. INTRODUCTION

CHANNEL estimation plays a crucial role in enhancing wireless communication systems. Recently, ML approaches were successfully leveraged for channel estimation. The goal is to exploit a priori information about all possible channels of mobile terminals (MTs) associated with a specific BS cell and its radio propagation environment, cf. Fig. 1, to improve the channel estimation quality. This is generally intractable to model analytically but is represented in terms of a training dataset that is available at the BS.

Thereby, different learning techniques can be distinguished. In end-to-end learning, the channel estimation is not performed explicitly, but a network is trained to directly perform signal detection [1]. A different approach is to learn a nonlinear regression mapping from the pilot observation in the input to a channel estimate at the output of a network by utilizing ground-truth CSI as labels [2], [3]. In contrast to that, it was recently proposed to train a generative model that represents the channel distribution of the whole BS cell, which is afterwards leveraged for channel estimation [4], [5].

A common prerequisite of ML-based approaches is the availability of a representative training dataset consisting of perfect CSI labels. However, the construction of such a dataset

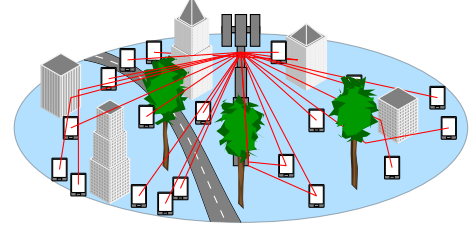


Fig. 1. Visualization of an urban radio propagation environment of a BS cell. The different links of the MTs are highlighted in red.

is a challenging task in practice. One possibility is to perform costly measurement campaigns for each BS, which is generally unaffordable. A different attempt is to use channel simulators, e.g., [6]. The inherent problem of simulators is the mismatch between the real and the adversarially generated data, leading to irreversible performance losses. Another problem is that the BS environment may change over time which is difficult to track. This leads to the idea of utilizing pilot observations, which are received in great numbers at the BS during regular operation and capture the environmental information, as training data. Although the data aggregation is then cheap and the dataset can be continuously updated to account for varying conditions, the dataset contains imperfections, e.g., noise and sparse pilot allocations. However, these imperfections can be mitigated by specific training adaptations since they follow a known model.

Contributions: In this letter, we propose an adaptation of the EM algorithm to fit a GMM with noisy, and possibly sparsely allocated, pilot observations. We derive new update steps for the GMM parameters that take the system model, i.e., the model of the imperfections, into account. Additionally, we show that imposing structural features to the covariances of the GMM acts as a regularization which enhances the channel estimation performance, especially for sparse pilot allocations. It is discussed that the concept of a generative model which is used for channel estimation is particularly robust against imperfections in the training data, in contrast to commonly used regression-based ML techniques. Finally, the discussed properties are verified with simulations for both a spatial and a doubly-selective fading model.

II. SYSTEM AND CHANNEL MODELS

We consider the generic system model of pilot observations

$$\mathbf{y} = \mathbf{A}\mathbf{h} + \mathbf{n} \quad (1)$$

This work was partly funded by Huawei Sweden Technologies AB, Lund. The authors are with Professur für Methoden der Signalverarbeitung, Technische Universität München, 80333 München, Germany (e-mail: benedikt.fesl@tum.de; nurettin.turan@tum.de; joham@tum.de; utschick@tum.de).

where \mathbf{A} is the known observation matrix, $\mathbf{h} \in \mathbb{C}^N$ is the wireless channel with unknown distribution $f_{\mathbf{h}}$, and additive white Gaussian noise (AWGN) $\mathbf{n} \sim \mathcal{N}_{\mathbb{C}}(\mathbf{0}, \mathbf{C}_n = \sigma^2 \mathbf{I})$. In this letter, we consider the following two instances of (1).

A. Spatial System Model

Consider a single-input multiple-output (SIMO) system where a BS equipped with N antennas serves single-antenna MTs in an uplink transmission. Thus, the observation matrix $\mathbf{A} = \mathbf{I}$ in (1) without loss of generality.

We work with a spatial channel model [3] where channels are modeled conditionally Gaussian: $\mathbf{h}|\delta \sim \mathcal{N}_{\mathbb{C}}(\mathbf{0}, \mathbf{C}_\delta)$. The random vector δ collects the angles of arrival and path gains of the main propagation clusters between a MT and the BS. A different spatial channel covariance matrix \mathbf{C}_δ is computed for each sample by means of the steering vector of a uniform linear array (ULA) antenna array at the BS, cf. [3].

B. Doubly-Selective Fading System Model

In this case, we consider a single-input single-output (SISO) transmission in the spatial domain over a doubly-selective fading channel, where $\mathbf{H} \in \mathbb{C}^{N_c \times N_t}$ represents the time-frequency response of the channel for N_c carriers and N_t time slots. This is a typical setup in orthogonal frequency-division multiplexing (OFDM) systems. When only N_p positions of the $N_t \times N_c$ time-frequency response are occupied by pilot symbols, there is a *selection matrix* $\mathbf{A} \in \{0, 1\}^{N_p \times N_c N_t}$ which represents the pilot positions. This leads to pilot observations as described in (1) where $N = N_c N_t$. In this work, we consider a diamond-shaped pilot allocation scheme which is known to be mean square error (MSE)-optimal [7].

For the construction of a scenario-specific channel dataset, we use the QuaDRiGa channel simulator [6]. We consider an urban macrocell (UMa) scenario following the 3GPP 38.901 specification, where the BS is placed at a height of 25m and covers a sector of 120°. Each MT is either placed indoors (80%) or outdoors (20%) and moves with a certain velocity v in a random direction, which is captured by a drifting model.

III. LEARNING A GMM FROM IMPERFECT DATA

A. Scenario-Specific Imperfect Training Dataset

Having access to training data that represent the environment of a BS cell as depicted in Fig. 1, i.e., the typically complex and intractable distribution of channels, in combination with ML techniques, has been shown to substantially improve the channel estimation performance. The common prerequisite of these data-aided techniques is the availability of a training dataset \mathcal{H} consisting of perfect CSI labels, i.e., L channel realizations $\mathcal{H} = \{\mathbf{h}_\ell\}_{\ell=1}^L$. However, this assumption is impractical if the training data are collected at a BS during regular operation. That is, the training data stem from certain pilot positions at a finite signal-to-noise ratio (SNR), i.e., $\mathcal{Y} = \{\mathbf{y}_\ell\}_{\ell=1}^L$, cf. (1). Note that these data can be pre-processed in different ways, e.g., by denoising or interpolating

the pilot positions. Although these training data is corrupted by various imperfections, the statistical information about the system model can be utilized to mitigate these effects, as shown in the following.

B. GMM based Channel Estimator with Adapted Training

In [4], a channel estimator was introduced that is based on a GMM whose application consists of two phases. First, in an offline training phase a K -components GMM of the form

$$f_{\mathbf{h}}^{(K)}(\mathbf{h}) = \sum_{k=1}^K \pi_k \mathcal{N}_{\mathbb{C}}(\mathbf{h}; \boldsymbol{\mu}_k, \mathbf{C}_k) \quad (2)$$

is fitted by maximum likelihood optimization with the help of the well-known EM algorithm, cf. [8, Sec. 9.2], via training samples from \mathcal{H} in order to approximate the underlying distribution $f_{\mathbf{h}}$ of the channels in the whole BS cell. Second, the trained GMM is leveraged to perform channel estimation by computing a convex combination of linear minimum mean square error (MMSE) estimates for a given pilot signal \mathbf{y} , i.e.,

$$\hat{\mathbf{h}}_{\text{GMM}} = \sum_{k=1}^K \gamma_k(\mathbf{y}) \left(\mathbf{C}_k \mathbf{A}^H \mathbf{C}_{\mathbf{y},k}^{-1} (\mathbf{y} - \mathbf{A} \boldsymbol{\mu}_k) + \boldsymbol{\mu}_k \right) \quad (3)$$

where $\gamma_k(\mathbf{y})$ is the responsibility of the k th component and $\mathbf{C}_{\mathbf{y},k} = \mathbf{A} \mathbf{C}_k \mathbf{A}^H + \mathbf{C}_n$, cf. (1). In [9], the estimator was extended to impose structural features to the covariances \mathbf{C}_k in the training of the GMM for saving complexity and memory.

However, so far, the GMM was trained on a dataset comprised of perfect channels \mathcal{H} , cf. Section III-A. If we naively replace \mathcal{H} with the noisy, possibly pre-processed, training data \mathcal{Y} from pilot observations (1), a severe performance loss can be expected due to the imperfections in the training data. Therefore, in the following, we propose adapted training procedures for the GMM that drastically alleviates the effects of the imperfect training data by utilizing the knowledge of the system model (1) and possibly existing structural features of the covariances.

We first discuss the case of training data that is corrupted by AWGN following the model in (1) with $\mathbf{A} = \mathbf{I}$, cf. Section II-A. The main idea is to adapt the EM algorithm such that the distribution $f_{\mathbf{y}}$ of the observations is approximated by the GMM, i.e., $f_{\mathbf{y}}^{(K)}(\mathbf{y}) = \sum_{k=1}^K \pi_k \mathcal{N}_{\mathbb{C}}(\mathbf{y}; \boldsymbol{\mu}_k, \mathbf{C}_{\mathbf{y},k})$. Since the mixing coefficients π_k and the means $\boldsymbol{\mu}_k$ (due to zero-mean AWGN) are not affected, their updates are unchanged with respect to the classical EM algorithm, cf. [8, Sec. 9.2]. However, we would like to include the constraint that $\mathbf{C}_{\mathbf{y},k} = \mathbf{C}_k + \mathbf{C}_n$, following the model (1). The GMM for the channel distribution (2) can then be directly obtained since \mathbf{C}_n is known. The derivation for the update of \mathbf{C}_k is given in the following.

Theorem 1. *Given noisy pilot observations \mathcal{Y} , the maximum likelihood solution \mathbf{C}_k^* for the covariance in the EM algorithm is given by computing the eigenvalue decomposition (EVD)*

$$\hat{\mathbf{C}}_{\mathbf{y},k} - \mathbf{C}_n = \mathbf{V} \text{diag}(\boldsymbol{\xi}) \mathbf{V}^H \quad (4)$$

with $\hat{\mathbf{C}}_{\mathbf{y},k} = \frac{1}{N_k} \sum_{\ell=1}^L \gamma_{k,\ell} (\mathbf{y}_\ell - \boldsymbol{\mu}_k)(\mathbf{y}_\ell - \boldsymbol{\mu}_k)^H$, $N_k = \sum_{\ell=1}^L \gamma_{k,\ell}$, and $\gamma_{k,\ell}$ being the responsibility of component k for data point \mathbf{y}_ℓ . Afterwards, an elementwise truncation of the negative eigenvalues via $\boldsymbol{\xi}^{PSD} = \max(\mathbf{0}, \boldsymbol{\xi})$ is performed such that

$$\mathbf{C}_k^* = \mathbf{V} \text{diag}(\boldsymbol{\xi}^{PSD}) \mathbf{V}^H. \quad (5)$$

Proof. The maximization of the expected complete log-likelihood, cf. [8, Sec. 9.3], of the pilot observations with respect to the k th channel covariance \mathbf{C}_k is given by

$$\begin{aligned} \mathbf{C}_k^* &= \arg \max_{\mathbf{C}_k \succeq \mathbf{0}} \sum_{j=1}^K \sum_{\ell=1}^L \gamma_{j,\ell} \log \mathcal{N}_{\mathbb{C}}(\mathbf{y}_\ell; \boldsymbol{\mu}_j, \mathbf{C}_j + \mathbf{C}_n) \\ &= \arg \max_{\mathbf{C}_k \succeq \mathbf{0}} \sum_{\ell=1}^L \gamma_{k,\ell} \log \mathcal{N}_{\mathbb{C}}(\mathbf{y}_\ell; \boldsymbol{\mu}_k, \mathbf{C}_k + \mathbf{C}_n) \\ &= \arg \max_{\mathbf{C}_k \succeq \mathbf{0}} -\log \det(\mathbf{C}_k + \mathbf{C}_n) - \text{tr}(\hat{\mathbf{C}}_{\mathbf{y},k}(\mathbf{C}_k + \mathbf{C}_n)^{-1}) \end{aligned}$$

which simplifies to a maximization of the Gaussian likelihood of the k th GMM component. The optimal solution for the case of a Gaussian likelihood is derived in [10, Appendix] and is obtained with the EVD and the truncation of the negative eigenvalues. This can be applied to the above simplified maximization problem through a substitution of the weighted sample covariance $\hat{\mathbf{C}}_{\mathbf{y},k}$ which yields the solution in (5). \square

In the following, the case of training data that stem from noisy pilot observations where only a few channel entries are observed according to a specific pilot pattern, cf. Section II-B, is discussed. In order to adapt the training procedure for this case, we combine the insights from the pure AWGN case in Theorem 1 together with the adapted EM algorithm for missing entries, cf. [11, Chapter 11]. Let us first define a selection matrix $\bar{\mathbf{A}}$ which represents the positions that are not allocated with pilots, i.e., $\mathbf{A}\bar{\mathbf{A}}^T = \mathbf{0}$. After an initial interpolation step, e.g., linear interpolation, one EM iteration is performed in the usual way to have initial estimates of the GMM parameters. The adapted updates of the GMM channel covariances are derived in the following.

Theorem 2. *Given sparsely allocated and noisy pilot observations \mathcal{Y} , first, a linear MMSE estimate of the unobserved and noisy channel entries $\bar{\mathbf{y}}_{k,\ell}$ is computed via the current statistics of the k th GMM component as*

$$\bar{\mathbf{y}}_{k,\ell} = \bar{\mathbf{A}}\boldsymbol{\mu}_k + \bar{\mathbf{A}}\mathbf{C}_k\mathbf{A}^T(\mathbf{A}\mathbf{C}_k\mathbf{A}^T + \mathbf{C}_n)^{-1}(\mathbf{y}_\ell - \mathbf{A}\boldsymbol{\mu}_k). \quad (6)$$

Afterwards, a fully interpolated sample, given as $\hat{\mathbf{y}}_{k,\ell} = \mathbf{A}^T\mathbf{y}_\ell + \bar{\mathbf{A}}^T\bar{\mathbf{y}}_{k,\ell}$, is used to update

$$\hat{\mathbf{C}}_{\mathbf{y},k} = \frac{1}{N_k} \sum_{\ell=1}^L \gamma_{k,\ell} (\hat{\mathbf{y}}_{k,\ell} - \boldsymbol{\mu}_k)(\hat{\mathbf{y}}_{k,\ell} - \boldsymbol{\mu}_k)^H + \bar{\mathbf{A}}^T \boldsymbol{\Sigma}_k \bar{\mathbf{A}} \quad (7)$$

where $N_k = \sum_{\ell=1}^L \gamma_{k,\ell}$ and

$$\boldsymbol{\Sigma}_k = \bar{\mathbf{A}}\mathbf{C}_k\bar{\mathbf{A}}^T - \bar{\mathbf{A}}\mathbf{C}_k\mathbf{A}^T(\mathbf{A}\mathbf{C}_k\mathbf{A}^T + \mathbf{C}_n)^{-1}\mathbf{A}\mathbf{C}_k\bar{\mathbf{A}}^T. \quad (8)$$

Finally, to account for the AWGN, the update of the channel covariance matrix \mathbf{C}_k is computed via the EVD of $\hat{\mathbf{C}}_{\mathbf{y},k} - \mathbf{C}_n$ and the projection via the truncation of the negative eigenvalues as shown in Theorem 1.

Proof. The steps (6)-(8) are derived in the EM algorithm for missing data, cf. [11, Chapter 11], where the additional covariance term (8) accounts for the estimated covariance of the missing entries. The subsequent projection via the EVD is a direct consequence of Theorem 1. \square

Additionally, it is possible to enforce covariances with a specific structure. For the derivation of these approaches we refer to [9]. In this letter, we are focusing especially on the case of block-Toeplitz covariances, constructed as $\mathbf{C}_k = \mathbf{Q}^H \text{diag}(c_k) \mathbf{Q}$, where \mathbf{Q} is a truncated 2D-discrete Fourier transform (DFT) matrix. This structure fits particularly well in the OFDM case [9]. It is important to mention that the imposed structural constraints on the covariances can be understood as a regularization technique. Interestingly, as shown later in Section IV, this regularization allows for performance gains, especially in the case of sparse pilot allocations.

Algorithm 1 summarizes the proposed adapted EM algorithm for fitting the GMM in the OFDM case with noisy and sparsely allocated pilot observations with structured covariances. It has to be noted that if we consider the pure AWGN case with $\mathbf{A} = \mathbf{I}$, the steps 8, 9, and 14 can be omitted. For the unconstrained case, the steps 2, 20, 21, and 22 are dropped.

C. Discussion about Robustness

The first stage of training the GMM is equivalent to learn a generative model that represents the channel distribution of the whole BS cell, cf. Fig. 1. On the one hand, this generative model allows to leverage prior information about the distribution of the channels in the whole BS cell that enhances the channel estimation performance [4]. On the other hand, it can be adapted to imperfections in the training data as discussed above which is motivated by model-based insights. This is a fundamental difference to common learning-based estimators that are trained to learn a nonlinear mapping between pilot observations and channel estimates, which inherently rely on perfect CSI as training labels, e.g., [1]–[3]. Thus, the proposed GMM approach allows for a more robust solution with respect to various imperfections in the training data because of its ability to adapt the training procedure accordingly and introduce structural regularization, cf. Section III-B. This is confirmed by simulations in Section IV.

An important advantage of the GMM estimator is the fact that only the training phase must be changed in contrast to [4] where perfect training CSI is assumed to be available. Thus, the online complexity and the number of parameters of the estimator do not change. Furthermore, the estimated GMM is universal and requires further adaptation only in case of changing parameters of the whole propagation environment which can be conveniently tracked with the frequently received pilots at the BS. Additionally, it has to be trained only once for a given SNR and can then be applied to any other SNR value, which is in contrast to learning-based estimators where the dependency on the SNR is crucial, e.g., [2], [3].

Fortunately, since the proposed covariance updates in Theorem 1 and Theorem 2 are indeed the maximum likelihood

Algorithm 1 Adapted EM with Structured Covariances.

Require: \mathcal{Y} , K , \mathbf{A} , \mathbf{C}_n , $\{\boldsymbol{\mu}_k^{(1)}, \mathbf{C}_k^{(1)}, \pi_k^{(1)}\}_{k=1}^K$, \mathbf{Q} , $i = 1, i_{\max}$

```

1: Get selection matrix  $\bar{\mathbf{A}}$  such that  $\bar{\mathbf{A}}\bar{\mathbf{A}}^T = \mathbf{0}$ 
2: Initialize  $\{\mathbf{c}_k^{(1)} \leftarrow \mathbf{Q}\mathbf{C}_k^{(1)}\mathbf{Q}^H\}_{k=1}^K$ 
3: while  $i < i_{\max}$  and convergence criterion not met do
4:    $\{\mathbf{C}_{\mathbf{y},k}^{(i)} \leftarrow \bar{\mathbf{A}}\mathbf{C}_k^{(i)}\bar{\mathbf{A}}^T + \mathbf{C}_n\}_{k=1}^K$ 
5:   for  $k = 1$  to  $K$  do
6:     for  $\ell = 1$  to  $L$  do
7:        $\gamma_{k,\ell} \leftarrow \frac{\pi_k^{(i)} \mathcal{N}_{\mathbf{C}}(\mathbf{y}_\ell; \mathbf{A}\boldsymbol{\mu}_k^{(i)}, \mathbf{C}_{\mathbf{y},k}^{(i)})}{\sum_{j=1}^K \pi_j^{(i)} \mathcal{N}_{\mathbf{C}}(\mathbf{y}_\ell; \mathbf{A}\boldsymbol{\mu}_j^{(i)}, \mathbf{C}_{\mathbf{y},j}^{(i)})}$  {E-step}
8:        $\hat{\mathbf{y}}_{k,\ell} \leftarrow \bar{\mathbf{A}}\boldsymbol{\mu}_k^{(i)} + \bar{\mathbf{A}}\mathbf{C}_k^{(i)}\bar{\mathbf{A}}^T \mathbf{C}_{\mathbf{y},k}^{(i),-1}(\mathbf{y}_\ell - \mathbf{A}\boldsymbol{\mu}_k^{(i)})$ 
9:        $\hat{\mathbf{y}}_{k,\ell} \leftarrow \mathbf{A}^T \mathbf{y}_\ell + \bar{\mathbf{A}}^T \hat{\mathbf{y}}_{k,\ell}$  {interpolated sample}
10:    end
11:     $N_k \leftarrow \sum_{\ell=1}^L \gamma_{k,\ell}$ 
12:     $\pi_k^{(i+1)} \leftarrow \frac{N_k}{L}$  {mixing coefficient update}
13:     $\boldsymbol{\mu}_k^{(i+1)} \leftarrow \frac{1}{N_k} \sum_{\ell=1}^L \gamma_{k,\ell} \hat{\mathbf{y}}_{k,\ell}$  {mean update}
14:     $\boldsymbol{\Sigma}_k \leftarrow \bar{\mathbf{A}}\mathbf{C}_k^{(i)}\bar{\mathbf{A}}^T - \bar{\mathbf{A}}\mathbf{C}_k^{(i)}\bar{\mathbf{A}}^T \mathbf{C}_{\mathbf{y},k}^{(i),-1} \mathbf{C}_{\mathbf{y},k}^{(i)}\bar{\mathbf{A}}^T$ 
15:     $\hat{\mathbf{y}}_{k,\ell} \leftarrow \hat{\mathbf{y}}_{k,\ell} - \boldsymbol{\mu}_k^{(i+1)}$ 
16:     $\mathbf{C}_{\mathbf{y},k}^{(i+1)} \leftarrow \frac{1}{N_k} \sum_{\ell=1}^L \gamma_{k,\ell} \hat{\mathbf{y}}_{k,\ell} \hat{\mathbf{y}}_{k,\ell}^H + \bar{\mathbf{A}}^T \boldsymbol{\Sigma}_k \bar{\mathbf{A}}$ 
17:     $\mathbf{V}_k, \boldsymbol{\xi}_k \leftarrow \text{EVD}(\mathbf{C}_{\mathbf{y},k}^{(i+1)} - \mathbf{C}_n)$ 
18:     $\boldsymbol{\xi}_k^{\text{PSD}} \leftarrow \max(\mathbf{0}, \boldsymbol{\xi}_k)$  {elementwise max}
19:     $\mathbf{C}_k^{(i+1)} \leftarrow \mathbf{V}_k \text{diag}(\boldsymbol{\xi}_k^{\text{PSD}}) \mathbf{V}_k^H$ 
20:     $\boldsymbol{\Theta}_k \leftarrow \mathbf{Q} \left( \mathbf{C}_k^{(i),-1} \mathbf{C}_k^{(i+1)} \mathbf{C}_k^{(i),-1} - \mathbf{C}_k^{(i),-1} \right) \mathbf{Q}^H$ 
21:     $\mathbf{c}_k^{(i+1)} \leftarrow \mathbf{c}_k^{(i)} + \text{diag} \left( \text{diag}(\mathbf{c}_k^{(i)}) \boldsymbol{\Theta}_k \text{diag}(\mathbf{c}_k^{(i)}) \right)$ 
22:     $\mathbf{C}_k^{(i+1)} \leftarrow \mathbf{Q}^H \text{diag}(\mathbf{c}_k^{(i+1)}) \mathbf{Q}$  {covariance update}
23:  end
24:   $i \leftarrow i + 1$ 
25: end
26: return  $\{\boldsymbol{\mu}_k^{(i)}, \mathbf{C}_k^{(i)}, \pi_k^{(i)}\}_{k=1}^K$ 

```

solutions, all favorable properties of the EM algorithm, such as a monotonically increasing likelihood, are preserved.

IV. SIMULATION RESULTS

In this section, we present numerical results to evaluate the proposed method for two different channel models in comparison to state-of-the-art estimators. We set $\mathbb{E}[\|\mathbf{h}\|^2] = N$ such that the $\text{SNR} = 1/\sigma^2$ and we choose $K = 64$. We utilize $L = 10^5$ training samples and evaluate on 10^4 test samples.

A. Spatial Channel Model

In this section, we evaluate the channel estimation performance for the spatial model from Section II-A with $\mathbf{A} = \mathbf{I}$. The GMM estimator which is based on perfect CSI is denoted by “GMM \mathcal{H} ”, whereas the GMM estimator that is naively used without any modifications on training data from \mathcal{Y} is denoted by “GMM mismatch”. The proposed approach with adapted training from Section III-B is denoted by “GMM \mathcal{Y} ”. We analyze the performance in comparison with several baseline estimators which are explained briefly in the following. The curve labeled “genie” represents the utopian MMSE estimator that has full knowledge of \mathbf{C}_δ for each sample.

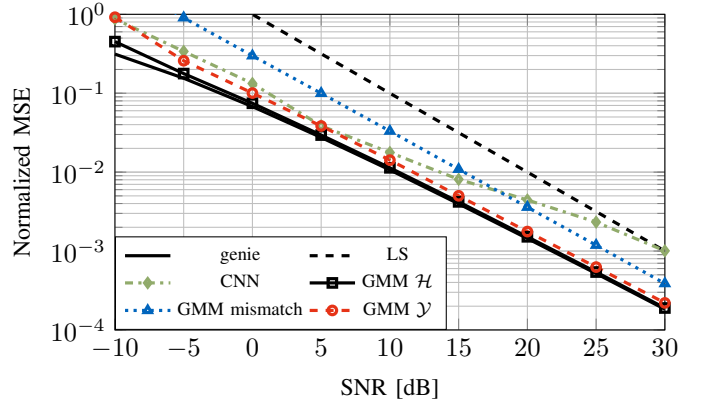


Fig. 2. Spatial channel model from Section II-A with $N = 128$ BS antennas and one propagation cluster. The SNR is the same for training and evaluation.

We further evaluate the least squares (LS) solution $\hat{\mathbf{h}}_{\text{LS}} = \mathbf{y}$. We include the ML-based estimator from [3], that treats the mapping between pilot observation and channel estimate as an unknown nonlinear function that is approximated via a convolutional neural network (CNN), labeled “CNN”. To achieve a fair comparison, the CNN estimator is trained on data that purely stem from \mathcal{Y} , which clearly introduces an unavoidable mismatch in the learning phase.

In Fig. 2, the channel estimation performance of the above discussed estimators is shown for $N = 128$ BS antennas and one propagation cluster, consisting of multiple sub-paths. The depicted SNR is the same in both training and evaluation, i.e., a different set of training data \mathcal{Y} is given for each SNR value, which mimics a realistic situation. The GMM estimator with perfect CSI \mathcal{H} performs very close to the genie-MMSE estimator which is in accordance with the findings in [4]. If the GMM estimator is fitted naively with data from \mathcal{Y} without modifications to the training procedure, this leads to a severe performance loss of about 5dB for the whole SNR range. However, with the proposed modifications, a performance close to the perfect CSI case, and thus to the genie-MMSE estimator, is possible, purely based on training data from \mathcal{Y} . The CNN estimator has a substantial performance loss as compared to the proposed estimator, especially in the high SNR regime.

B. Doubly-Selective Fading Channel Model

We consider a typical OFDM frame structure of $N_c = 12$ carriers having a spacing of 15kHz, yielding a bandwidth of 180kHz, and $N_t = 14$ time slots. We consider MTs which move with a uniform at random sampled velocity between three and 130km/h, i.e., $v \sim \mathcal{U}(3, 130)$ km/h. We evaluate once again the GMM estimator with perfect CSI from \mathcal{H} and a naive version where the GMM is fitted with linearly interpolated data from \mathcal{Y} , labeled “GMM lin-int”. The proposed approach with adapted training from Section III-B and linear interpolation as initialization is denoted by “GMM \mathcal{Y} ”. In the OFDM case, we can impose structural features to the covariances as regularization on the adapted approach. In this letter, we focus on block-Toeplitz matrices as discussed in [9], labeled

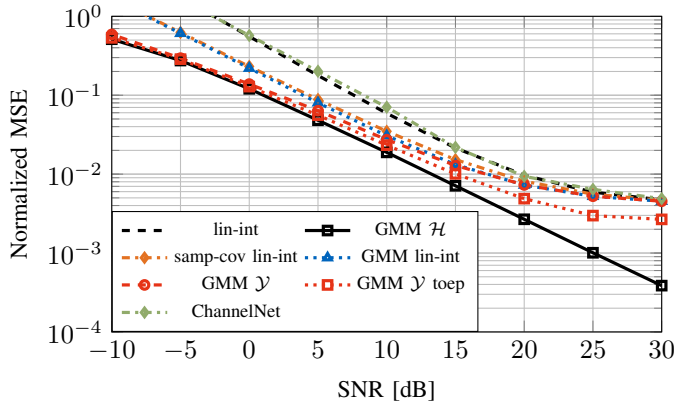


Fig. 3. Doubly-selective fading channel model from Section II-B with $N_c = 12$ carriers, $N_t = 14$ time symbols, $v \sim \mathcal{U}(3, 130)$ km/h, and $N_p = 18$ diamond-shaped pilots. The SNR is the same for training and evaluation.

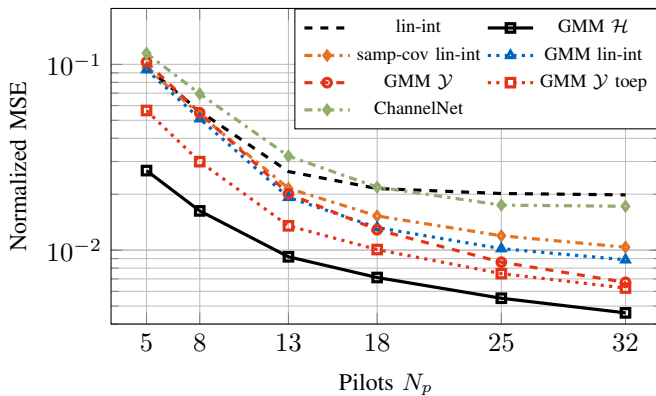


Fig. 4. Doubly-selective fading channel model from Section II-B with $N_c = 12$ carriers, $N_t = 14$ time symbols, $v \sim \mathcal{U}(3, 130)$ km/h, and SNR = 15 dB. The SNR is the same for training and evaluation.

as “GMM \mathcal{Y} toep”. We compare our proposed methods with the typically used linear interpolator, labeled “lin-int”, and with a linear MMSE estimator based on a cell-wide global sample covariance computed with linearly interpolated data from \mathcal{Y} , labeled as “samp-cov lin-int”. Note that this case the genie-MMSE estimator is not computable since no covariance statistics are provided from the simulator [6]. We also compare with the ML-based *ChannelNet* from [2] where the labels in the training are comprised of linearly interpolated data from \mathcal{Y} for a fair comparison.

In Fig. 3, the performances of the above discussed estimators are evaluated for $N_p = 18$ pilots over different SNR values. It can be seen that the *ChannelNet* has no performance improvement over linear interpolation, which is a consequence of the imperfect training data. The sample covariance and the naive GMM approach based on linearly interpolated training data exhibit some performance improvement over linear interpolation in the low and medium SNR range, whereas for high SNRs, an error floor because of the imperfections in the training data can be observed. The adapted GMM version without structural constraints is performing close to the perfect CSI case in the low SNR range, but also seems to saturate for high SNRs. In this SNR-region, the block-Toeplitz structured

adapted GMM performs especially well, showing performance gains over all other approaches even for high SNR values. This leads to the conclusion that the structural regularization, which is possible with the GMM, is of great value when having noisy training data with missing entries.

In Fig. 4, we show a similar setup as above for a fixed SNR of 15 dB over varying numbers of pilots. Thereby, linear interpolation and the *ChannelNet* perform worst with a saturation at a high error floor, which was similarly observed before. It can be seen that the differences between the sample covariance, naive GMM, and adapted (unconstrained) GMM become more distinctive for higher numbers of pilots where the adapted version is outperforming them and has a decreasing gap to the perfect CSI based GMM. This can be reasoned with a dominating systematic error for sparse pilot allocations. In contrast, the block-Toeplitz based adapted GMM shows a substantial performance gain over the baselines even for low numbers of pilots, which is an effect of the structural regularization. As expected, the difference between the structurally unconstrained and constrained adapted GMM decreases for higher numbers of pilots.

V. CONCLUSION

In this letter, a GMM-based robust channel estimator was proposed which can be applied in spatial and OFDM systems. Thereby, the training data are purely comprised of sparsely allocated and noisy pilot observations, without perfect CSI labels. We derived adapted training procedures of the underlying EM algorithm for both systems which mitigate the imperfections in the training data. Finally, we imposed beneficial structural constraints to the covariances of the GMM, which acts as a regularization.

Simulation results demonstrated that the performance of the proposed adapted GMM estimator is close to the version which utilizes perfect training CSI with the same online complexity and memory overhead. Additionally, state-of-the-art baselines are outperformed. Based on these findings, the superior robustness properties against imperfect training data of the generative model-aided estimator in contrast to regression-based ML approaches were discussed.

REFERENCES

- [1] H. Ye, G. Y. Li, and B.-H. Juang, “Power of Deep Learning for Channel Estimation and Signal Detection in OFDM Systems,” *IEEE Wireless Commun. Lett.*, vol. 7, no. 1, pp. 114–117, 2018.
- [2] M. Soltani, V. Pourahmadi, A. Mirzaei, and H. Sheikhzadeh, “Deep Learning-Based Channel Estimation,” *IEEE Commun. Lett.*, vol. 23, no. 4, pp. 652–655, 2019.
- [3] D. Neumann, T. Wiese, and W. Utschick, “Learning the MMSE Channel Estimator,” *IEEE Trans. Signal Process.*, vol. 66, no. 11, pp. 2905–2917, Jun. 2018.
- [4] M. Koller, B. Fesl, N. Turan, and W. Utschick, “An Asymptotically MSE-Optimal Estimator Based on Gaussian Mixture Models,” *IEEE Trans. Signal Process.*, vol. 70, pp. 4109–4123, 2022.
- [5] M. Baur, B. Fesl, M. Koller, and W. Utschick, “Variational Autoencoder Leveraged MMSE Channel Estimation,” in *56th Asilomar Conf. Signals, Syst., Comput.*, 2022.
- [6] S. Jaeckel, L. Raschkowski, K. Börner, and L. Thiele, “QuaDRiGa: A 3-D Multi-Cell Channel Model With Time Evolution for Enabling Virtual Field Trials,” *IEEE Trans. Antennas Propag.*, vol. 62, no. 6, pp. 3242–3256, 2014.

- [7] J.-W. Choi and Y.-H. Lee, "Optimum Pilot Pattern for Channel Estimation in OFDM Systems," *IEEE Trans. Wireless Commun.*, vol. 4, no. 5, pp. 2083–2088, Sep. 2005.
- [8] C. M. Bishop, *Pattern Recognition and Machine Learning (Information Science and Statistics)*. Berlin, Heidelberg: Springer-Verlag, 2006.
- [9] B. Fesl, M. Joham, S. Hu, M. Koller, N. Turan, and W. Utschick, "Channel Estimation based on Gaussian Mixture Models with Structured Covariances," in *56th Asilomar Conf. Signals, Syst., Comput.*, 2022.
- [10] D. Neumann, M. Joham, L. Weiland, and W. Utschick, "Low-Complexity Computation of LMMSE Channel Estimates in Massive MIMO," in *Proc. 19th Int. ITG Workshop Smart Antennas*, 2015.
- [11] R. J. A. Little and D. B. Rubin, *Statistical Analysis with Missing Data*. John Wiley & Sons, Incorporated, 2002.